Source Shape Determination with Directional Correlation Functions

A. Le Fèvre[1], C. Schwarz[1], G. Auger[2], M.L. Begemann-Blaich[1], N. Bellaize[3], R. Bittiger[1], F. Bocage[3], B. Borderie[4], R. Bougault[3], B. Bouriquet[2], J.L. Charvet[5], A. Chbihi[2], R. Dayras[5], D. Durand[3], J.D. Frankland[2], E. Galichet[4,11], D. Gourio[1], D. Guinet[6], S. Hudan[2], B. Hurst[3], P. Lautesse[6], F. Lavaud[4], R. Legrain[*,5], O. Lopez[3], J. Łukasik[1,10], U. Lynen[1], W.F.J. Müller[1], L. Nalpas[5], H. Orth[1], E. Plagnol[4], E. Rosato[7], A. Saija[8], C. Sfienti[1], J.C. Steckmeyer[3], B. Tamain[3], W. Trautmann[1], A. Trzciński[9], K. Turzó[1], E. Vient[3], M. Vigilante[7], C. Volant[5], B. Zwiegliński[9] and A.S. Botvina[1,12].
(The INDRA and ALADIN Collaborations)

[1] Gesellschaft für Schwerionenforschung mbH, D-64291 Darmstadt, Germany.
[2] GANIL, CEA et IN2P3-CNRS, F-14076 Caen, France.
[3] LPC, IN2P3-CNRS, ISMRA et Université, F-14050 Caen, France.
[4] Institut de Physique Nucléaire, IN2P3-CNRS et Université, F-91406 Orsay, France.
[5] DAPNIA/SPhN, CEA/Saclay, F-91191 Gif sur Yvette, France.
[6] Institut de Physique Nucléaire, IN2P3-CNRS et Université, F-69622 Villeurbanne, France.
[7] Dipartimento di Scienze Fisiche e Sezione INFN, Univ. Federico II, I-80126 Napoli, Italy.
[8] Dipartimento di Fisica dell' Università and INFN, I-95129 Catania, Italy.
[9] A. Sołtan Institute for Nuclear Studies, PL-00681 Warsaw, Poland.
[10] H. Niewodniczański Institute of Nuclear Physics, PL-31342 Kraków, Poland.
[11] Conservatoire National des Arts et Métiers, F-75141 Paris cedex 03, France.
[12] Institute for Nuclear Research, 117312 Moscow, Russia.

Abstract

Non-isotropic effects have been observed in central collisions of ^{129}Xe+^{nat}Sn at 50 A.MeV and ^{197}Au+^{197}Au at 60, 80 and 100 A.MeV incident energies, measured with INDRA at GSI. In all reactions, anisotropy of the fragment distributions in size and mean kinetic energy indicate an incomplete shape relaxation of the multifragmenting source. Using the Berlin microcanonical multifragmentation model (MMMC) extended to a non-spherical source, we have shown that the standard assumption of a spherical source, expanding with either isotropic or anisotropic radial flow, cannot simultaneously explain the angular dependence of both the charge distributions and the fragment kinetic energies. This anisotropy can be understood as the consequence of the statistical multifragmentation of a prolate expanding source aligned along the beam direction. In order to improve the shape characterization of the source, we have constructed correlation functions between fragments from the projected relative velocities. Their sensitivity to various properties of the source like its geometry (volume and shape) has been tested in model studies using results from MMMC calculations. As compared to the correlation functions with angular cuts, the new method employing projections shows a higher sensitivity. The application to the experimental data confirms the spatial elongations of the sources that have previously been determined.

1 Introduction

Numerous transport calculations indicate that in central heavy-ion collisions at intermediate energies, significant compression and heating of nuclear matter occur in the initial stage of the reaction (see e.g. [1, 2]). The hot and compressed matter subsequently expands

[*] deceased

resulting in a dynamical instability leading to multifragmentation, i.e. to the formation of a large number of intermediate mass fragments. These fragments contain the imprints of both the initial temperature of the disassembling source and the flow energy stored initially in the compressed mode. Although this is initiated through a dynamical process, numerous studies (e.g. [3-11]) show that statistical models can successfully describe the product partitions, indicating that a high degree of thermalization has been achieved. Indeed, experimental results [8, 10, 12, 13] have revealed anisotropies in fragment emissions, in size and in kinetic energies. They suggest a non-complete shape relaxation of sources formed in heavy-ion central collisions at intermediate energies, which may originate from nuclear transparency. This implies that the statistical description may no longer be valid, requiring the partition space being filled in an expanding and non-spherical volume. The Berlin statistical multifragmentation model MMMC (for "Multifragmentation Metropolis Monte-Carlo", ref. [14]) extended to the case of non-spherical nuclei [12, 15], has shown that it is possible to describe the observed anisotropies. Within this model, they are explained by the non-sphericity of the source in coordinate space, at the low-density freeze-out stage. In order to obtain additional – qualitative and quantitative – evidence for such elongations, we have employed directional correlation functions, which have been extensively used to gain access to the space-time geometry of the final freeze-out stage [16-18].

2 The fragment anisotropies as explained by the statistical approach

From the recent results of the 4^{th} INDRA campaign at GSI, we have found that central collisions of heavy symmetric systems lead to the formation of a heavy, hot and expanding composite nucleus. It exhibits pronounced anisotropies in the fragment yields and kinetic energies, as observed in the ^{197}Au+^{197}Au and ^{129}Xe+^{nat}Sn systems studied in the energy range of 40 to 150 A.MeV [8]. Both break-up properties and anisotropies have been successfully reproduced [15] within the extension of the standard version of the Berlin statistical multifragmentation model to non-spherical sources (so-called MMMC-NS, for "MMMC-Non Spherical", ref. [12]).

As an illustration of the good agreement that we have obtained, we present in Figs. 1 and 2 the comparisons between the experimental data of central ^{197}Au+^{197}Au at 60 A.MeV and the MMMC-NS predictions, for the charge distributions and the mean kinetic energies of fragments, respectively. They are separately shown for two angular regions in the center-of-mass of the system (forwards and sidewards with regard to the beam direction). The central collisions have been selected by requiring that the total transverse energy of light charged particles ($Z = 1, 2$) $E_{\perp 12} \geq 1256$ MeV. This represents a reduced impact parameter $b/b_{max} \leq 0.1$, following the geometrical prescription [19]. The model predictions that we show correspond to the best agreement to the data. They have been obtained with a source having a prolate shape in the coordinate space, elongated along the beam axis, with a longitudinal-to-transversal elongation ratio $\mathcal{R} = (1 : 0.7)$. It has a size $Z_s = 125$, of excitation energy 6 A.MeV, of mean collective energy of radial flow 3.1 A.MeV, and a density $\rho \approx \rho_0/6$. The experimental data in Fig. 1 show that the forward charge distribution extends to much higher Z values and multiplicities than in sideward direction, indicating that forward emitted fragments are more numerous and bigger. In addition, Fig. 2 shows that these forward emitted fragments have much more kinetic energy.

Looking in particular at the largest fragment of each event, we observe in Figs. 3 and 4 that its mean size and kinetic energy increase monotonously from the transversal to the longitudinal directions. In all cases, the MMMC-NS predictions agree well with the

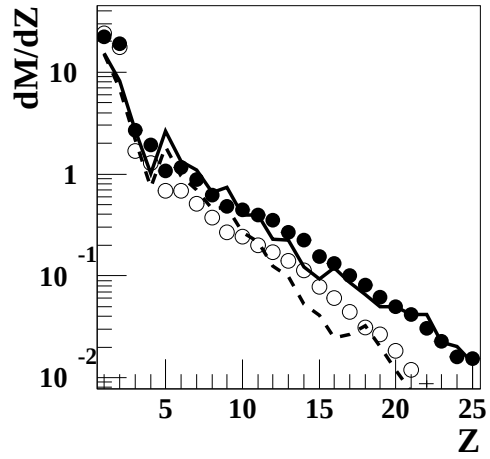

Figure 1: Mean multiplicities of fragment charges normalized to the total solid angle. The circles represent the experimental data (^{197}Au+^{197}Au at 60 $A.MeV$, central collisions), and the lines are the MMMC-NS model prediction obtained with the prolate source described in the text; the full circle and solid line account for forward angles (below 60^o around the beam in the center of mass); the open circle and the dashed line are for sideward angles (between 60^o and 120^o).

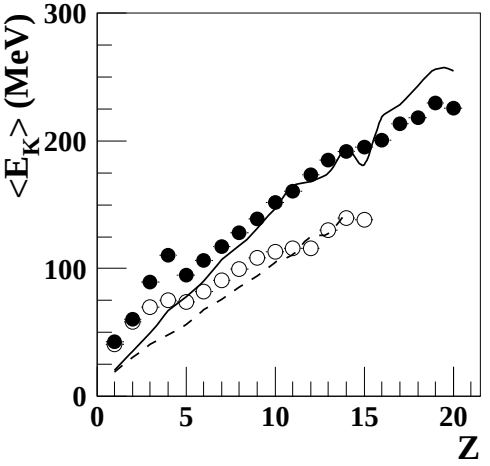

Figure 2: Mean kinetic energy of fragments as a function of Z in the center of mass, with the same notation as in Fig. 1.

experimental data. Within this model, a non-isotropic flow applied on a spherical source cannot explain the observed anisotropies: while it can provide the correct features of the fragment mean kinetic energies (shown in Figs. 2 and 4), it does not produce the observed anisotropies in fragment size (like in Figs. 1 and 3).

We have performed the same analysis for the ^{197}Au+^{197}Au central collisions at other beam energies, and for ^{129}Xe+^{nat}Sn at 50 A.MeV, measured during the 4^{th} INDRA campaign at GSI. We have deduced similar prolate deformations of the source in the coordinate space along the beam axis. Table 1 summarizes the source characteristics that we have determined. We observe that the elongation ratio $\mathcal{R}$ remains remarkably stable with the change in system size and beam energy, up to 80 A.MeV, while the size of the source, its excitation energy, and in particular its collective energy get strongly modified. It is only at 100 A.MeV that a more compact source is observed, which may indicate a decrease of the nuclear transparency around this energy.

In the MMMC-NS approach, the strong forward-backward focusing of the heaviest fragments originates from their particular location in the freeze-out volume, as illustrated in Fig. 5, middle panels. The transversal and longitudinal slice projections of the yields of heavy fragments ($Z > 4$) in the coordinate space at freeze-out show that the inner source space is strongly depleted, and heavy fragments are emitted predominantly from the tips of the ellipsoidal shape, not far from the boundary surface. We have noticed that this focusing is enhanced with increasing fragment charges. The light fragments

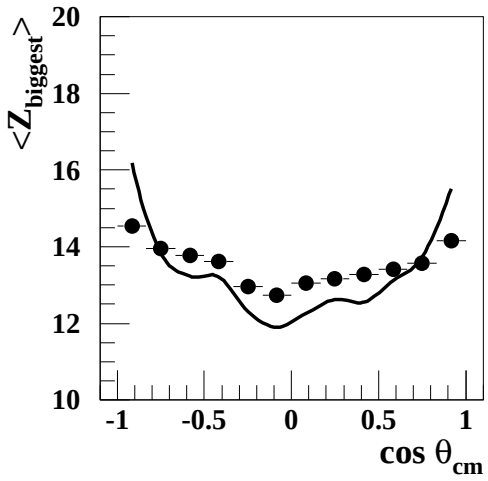

Figure 3: Angular distribution of the mean value of the biggest Z; the circles are the experimental data, the MMMC-NS model prolate source prediction is shown by the solid line; note the zero suppression on the ordinate.

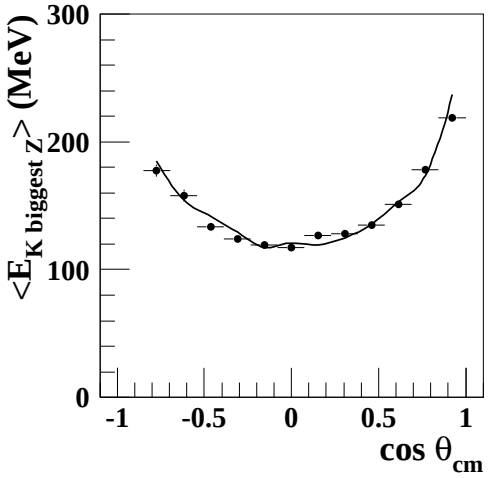

Figure 4: Mean kinetic energy of the biggest Z as a function of the angle; notation as in Fig. 3.

are more compactly distributed inside the source than the heavier ones. And the light charged particles (Z=1,2) are homogeneously distributed. We observe that the patterns of distributions in coordinate space – e.g. source geometry, ring structure in the transverse slice projection, forward/backward focusing – are transfered into the velocity space, as shown in the right panels of Fig. 5. This is induced by the radial collective flow which correlates directly with the fragment position (see [12]). This space-momentum correlation is slightly smeared out by the thermal motion.

In the framework of MMMC-NS, the correlation between the size of the fragment and its location in coordinate space is the consequence of the minimization of the Coulomb energy on the event-by-event basis. The Coulomb energy represents a major part of the total system energy. The total energy conservation, basic property of the microcanonical ensemble, puts essential constraints to the Coulomb energy at minimization. This gives small weight to the partitions with high Coulomb energy, in particular those where heavy fragments are compactly distributed in the freeze-out volume. As a result, the biggest fragments are preferentially emitted far away from the center, i.e. at the tips of the prolate source, giving the effects seen in Figs. 1-4. An illustration of the decisive role of the Coulomb energy is given in the left panels of Fig. 5 : if the Coulomb interaction is switched off, heavy fragments become homogeneously spread over the freeze-out volume (a slight increase of statistics around the surfaces is due the curved borders of the projected slices).

Table 1: Source characteristics at freeze-out measured in the central collisions from different reactions and deduced by means of the MMMC-NS model. From top to bottom, the quantities are: the beam energy, the energy of the system in the center-of-mass, and the charge, the mass, the prolate elongation ratio, the excitation energy and the mean collective flow energy of the source at freeze-out.

Reaction	^{129}Xe+^{nat}Sn	^{197}Au+^{197}Au		
E_0 (A.MeV)	50	60	80	100
E_{cm} (A.MeV)	13.4	14.9	19.8	24.7
Z_S	79 (76%)	125 (79%)	110 (70%)	95 (60%)
A_S	197	312	275	238
$\mathcal{R}$	(1:0.70)	(1:0.70)	(1:0.70)	(1:0.76)
E^* (A.MeV)	6.0	6.0	6.7	7.3
$< E_{coll} > (A.MeV)$	2.3	3.1	5.2	7.4

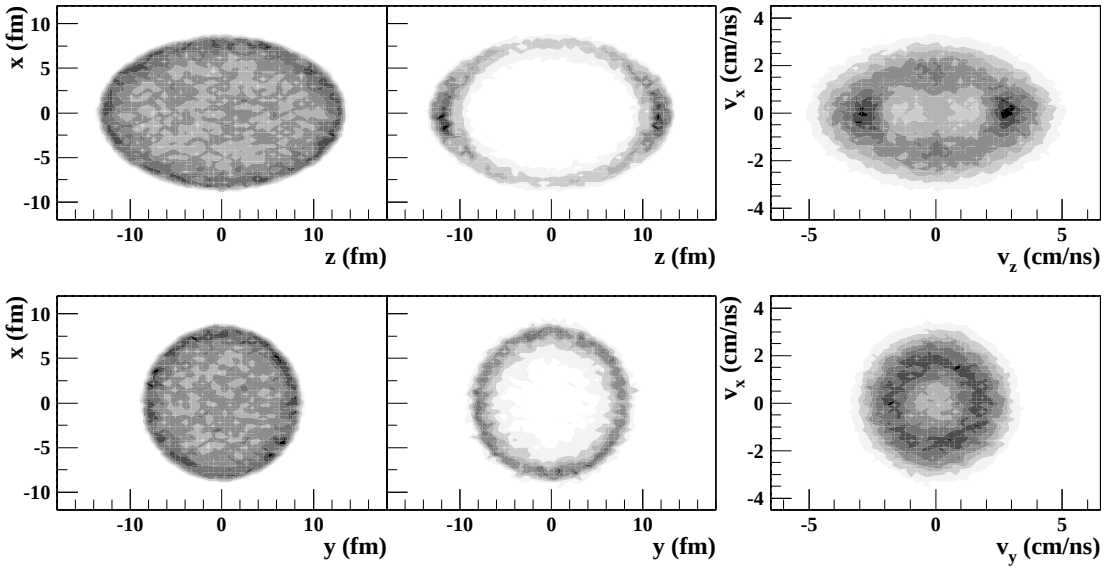

Figure 5: Two-dimensional distributions of fragments with $Z > 4$ obtained with the MMMC-NS prolate source prediction without INDRA filtering. Left: in coordinate space without Coulomb interaction. Middle: in coordinate space with Coulomb interaction. Right: in velocity space with Coulomb interaction. The top panels show the projections of longitudinal and centered slices, $5fm$ and $2cm/ns$ thick in coordinate and velocity space, respectively. The bottom panels show the same projections, but within a transversal slice (same thickness). The z-axis follows the beam, x and y-axis are perpendicular to the beam. The shading scale is linear.

3 Comparison of two methods of directional correlations

In order to obtain additional evidence for the geometrical properties of the composite system, we have get use of directional correlation functions in fragment relative velocity, in comparison with models. As a preliminary remark, we do not investigate the time degree of freedom, assuming that the multifragmentation in the present reactions is a prompt process, as it is supported by many experimental results (e.g. [17, 20, 21, 22, 23]).

3.1 Directional cuts

The first type of correlation function that we present is based on cuts on the angle ψ between the beam direction and the relative velocity of the particle pairs. Angular cuts have been suggested in [24] in order to study correlations between protons emitted with nearly equal momenta, for determining the size, velocity, and lifetime of the collision volume in heavy ion collisions at high energy. Instead of hard angular cuts, we have applied a harmonic *angular weight* for each event, like first introduced in [17]. We employed $cos^2(\psi)$ and $sin^2(\psi)$ as weights for the longitudinal and transversal correlation functions respectively. The correlation functions are constructed dividing the spectrum of reduced velocities of two coincident fragments by the spectrum of pairs from different events. The reduced velocity is defined as $v_{red} = v_{rel}/\sqrt{Z_1 + Z_2}$, where v_{rel}, Z_1 and Z_2 are the relative velocity and the charges of the two fragments, respectively. The angular weights are applied in both numerator and denominator spectra.

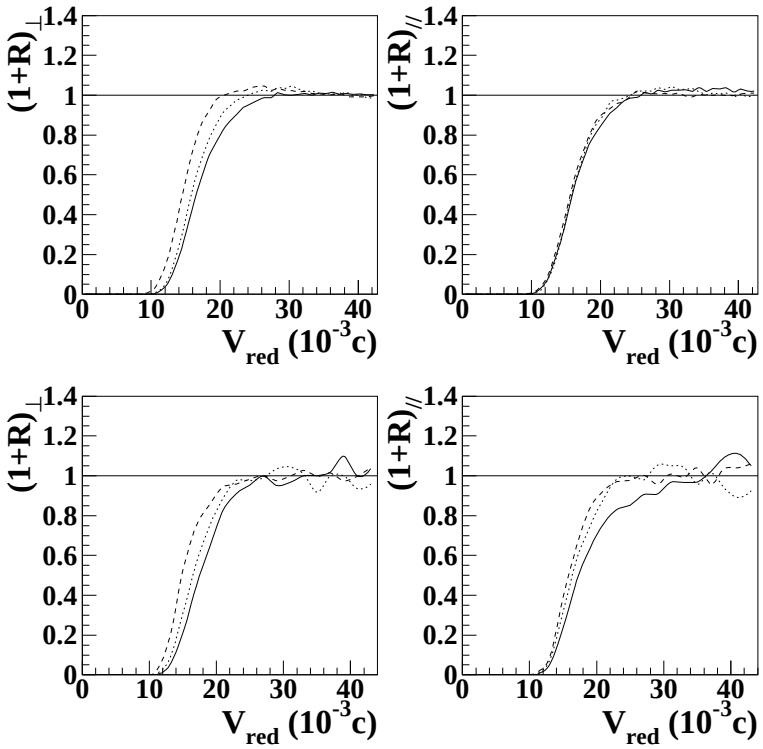

Figure 6: Correlation functions in reduced velocity between fragments pairs with $Z > 2$ (top panels) and between the two biggest fragments (bottom panels). Left and right panels correspond to the longitudinal and transversal correlation functions respectively, made by means of directional weights. The solid, dashed and dotted lines are the predictions of the MMMC-NS model for the prolate, oblate and spherical sources respectively.

In Fig. 6, MMMC-NS predictions with three different source elongations are presented: prolate, oblate – i.e. elongated/compressed along the beam with axis ratios 1:0.70 and 1:1.67 – and spherical, with a size Z=79, 6 A.MeV excitation energy and 2.3 A.MeV collective flow. The sensitivity of both directional correlation functions to the source elongation is seen on the width of their depletion at small v_{red}. The correlations between the

two biggest fragments of each event that are presented here give the strongest sensitivity within this model. This comes from the fact that, as explained in Section 2, the heavy fragments reflect the most the source elongation.

3.2 Directional projections

As a second type of correlation function, we have applied a new method. The correlation functions are generated for the longitudinal and the transversal *projections* – with regard to the beam axis – of the reduced velocity, i.e. $v_{red//} = v_{red} \cdot cos(\psi)$ and $v_{red\perp} = v_{red} \cdot sin(\psi)$ respectively. In Fig. 7, MMMC-NS predictions with the same three different source elongations as in Fig. 6 are shown. We observe that these functions exhibit a strong sensitivity to the source deformation, in the magnitude of their depletion at small v_{red}. Within this model, like for the directional cuts, the correlations between the two biggest fragments of each event give the strongest sensitivity. The comparison to the experimental data of ^{129}Xe+^{nat}Sn central collisions at 50 A.MeV shows, in both longitudinal and transversal projections, a good agreement with the prolate deformation that we had derived from the study of the fragment anisotropies in yields and kinetic energies. In particular, the experimental correlation functions exhibit higher depletions at small v_{red} for the heaviest fragments, in agreement with the MMMC-NS predictions. Following the model, this first suggests that the heaviest fragments are produced further from each other, which translates into a higher relative velocity through the radial flow. Second, this indicates that they have a stronger relative Coulomb repulsion, which happens when they are emitted from the surface of the freeze-out volume, in opposite directions.

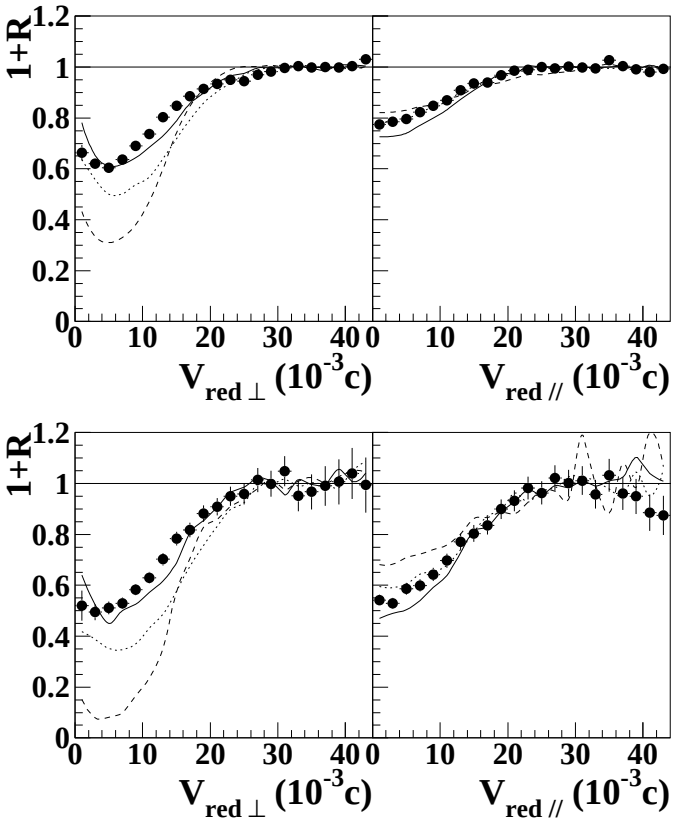

Figure 7: Correlation functions in projected reduced velocity between fragments with $Z > 2$ (top panels) and between the two biggest fragments (bottom panels). Left and right panels correspond to the longitudinal and transversal projections of the reduced velocity respectively. The lines are chosen like in Fig. 6. The symbols represent the experimental data of central ^{129}Xe+^{nat}Sn at 50 A.MeV.

3.3 Comparison of the two methods

In order to quantify the sensitivity of both types of directional correlation functions with the geometry of the source, we have simulated various volumes and deformations of ellipsoidal sources, following a simple model. The fragments are sampled according to the experimental distributions in yield and kinetic energy – including the angular dependences –, and placed randomly without overlap into the ellipsoidal "freeze-out" volume. The subsequent time evolution was modeled with N-body Coulomb trajectories. For each simulated source geometry, we have calculated the χ^2 corresponding to the comparison of the directional correlation functions with the experiment. Fig. 8 shows the resulting two-dimensional χ^2 distributions in the plane of the longitudinal and transversal extension of the source, obtained with fragments of $Z = 5 - 7$, compared to the data of central ^{129}Xe+^{nat}Sn at 50 A.MeV, for both angular cut and projection methods. With the directional cut method, we observe a fairly narrow valley of minimum χ^2 at constant volume, indicating a good sensitivity to the density of the source, but a weak sensitivity to the longitudinal to transversal radius ratio, i.e. to the elongation of the source in coordinate space. With the projection method, we observe a well defined and narrow χ^2 minimum that indicates a good sensitivity to both source density and shape in coordinate space. This minimum corresponds to a prolate source having a size ratio $1 : 0.6 \pm 0.1$ which is remarkably close to the MMMC-NS deduction for this reaction (see Table 1).

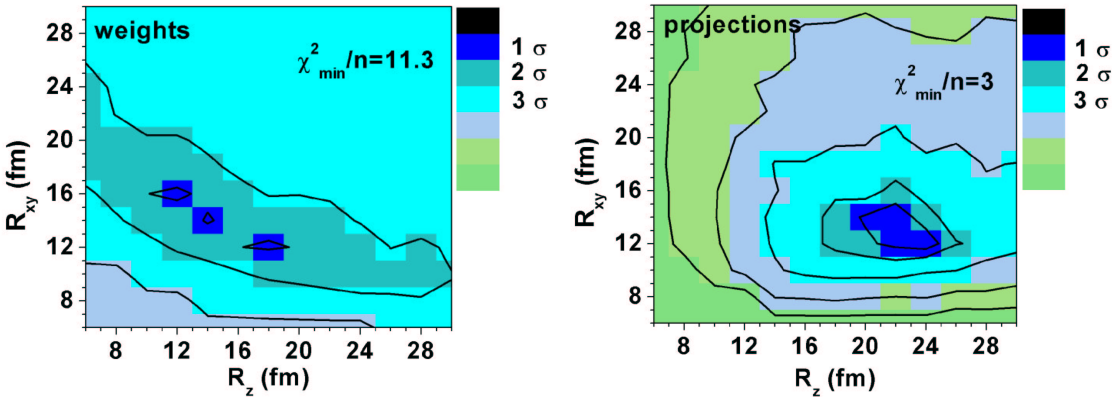

Figure 8: Contour plot (in units of the standard deviation σ) of the two-dimensional χ^2 distribution in the plane of the longitudinal (z) and transversal (xy) extension of the source, as obtained for the comparison of the directional correlation functions with fragments with $Z = 5 - 7$, from the experiment and from the N-body Coulomb trajectory calculations. The left panel correspond to the correlations with directional weights, and the right panel to the correlations in projected reduced velocities.

4 Summary and outlook

We have observed that in central collisions at intermediate energies, multifragmentation sources are formed that exhibit anisotropies in fragment sizes and kinetic energies. The statistical approach can describe them, along with their anisotropies, assuming non-spherical expanding sources, and allow to deduce their elongation in space.

Projected correlation functions in fragment reduced velocities, which yield at the same time information on volume – density – and elongation, confirm these predictions. Follow-

ing the MMMC-NS statistical approach, the correlations between the two largest fragments are the most sensitive to the spatial characteristics of the source, and exhibit the deepest depletions at small v_{red}, which is explained as an indirect effect of the Coulomb constraint in the conservation of the total energy of the system at freeze-out. In that respect, the effect of the radial flow has to be investigated.

We can interpret the observed sources elongations as the result of an incomplete stopping – i.e. transparency – of the colliding heavy ions, that has been observed at higher energies [25]. In particular, a recent study [26] as shown evidence for a strong increase of the nuclear stopping from 100 A.MeV to 400 A.MeV bombarding energy. The study of ^{197}Au+^{197}Au central collisions measured with INDRA at GSI indicates that this evolution prolongates down to the lower Fermi energy domain. The directional correlation functions seem to be an efficient tool to confirm and precise these findings.

References

[1] E. Suraud *et al.*, Phys. Lett. B **229**, 359 (1989), Nucl. Phys. A **495**, 73 (1989); Ph. Siemens and A.S. Jensen in *Elements of nuclei*, edited by Addison-Wesley, 1987, chap. 11.

[2] L. Neise *et al.*, Nucl. Phys. A **519**, 375 (1990); D.H. Boal *et al.*, Phys. Rev. C **40**, 601 (1989).

[3] R. Bougault *et al.*, in *Proceedings of the $XXXV^{th}$ International Winter Meeting on Nuclear Physics, Bormio, Italy, 1997*, edited by I. Iori, Ricerca Scientifica ed Educatione Permanente, Supplemento N. 110, 1997, p. 225.

[4] M. D'Agostino *et al.*, Phys. Lett. B **371**, 175 (1996).

[5] N. Bellaize *et al.*, Nucl. Phys. A **709**, 367 (2002).

[6] S. Hudan *et al.*, arXiv:nucl-ex/0210029; submitted to Phys. Rev. C.

[7] F. Lavaud *et al.*, in *Proceedings of the $XXXIX^{th}$ International Winter Meeting on Nuclear Physics, Bormio, Italy, 2001*, edited by I. Iori and A. Moroni, Ricerca Scientifica ed Educatione Permanente, Supplemento N. 117, 2001, p. 160.

[8] F. Lavaud, E.Plagnol *et al.*, in *Proceedings of the International Nuclear Physics Conference*, Berkeley, 2001, edited by E. Norman, L. Schroeder, G. Wozniak (LBNL, Berkeley, 2002), p.716.

[9] Al. H. Raduta and Ad. R. Raduta, Phys. Rev. C **65**, 2002 (054610)

[10] R. Nebauer, J. Aichelin and the INDRA collaboration, Nucl. Phys. A **658**, 67 (1999).

[11] C. Williams *et al.*, Phys. Rev. C **55**, R2132 (1997).

[12] A. Le Fèvre, M. Płoszajczak and V.D. Toneev, Phys. Rev. C **60**, 051602 (1999).

[13] B. Bouriquet *et al.*, in *Proceedings of the $XXXIX^{th}$ International Winter Meeting on Nuclear Physics, Bormio, Italy, 2001*, edited by I. Iori and A. Moroni, Ricerca Scientifica ed Educatione Permanente, Supplemento N. 117, 2001, p. 84.

[14] D.H.E. Gross, Rep. Prog. Phys. **53**, 605 (1990).

[15] A. Le Fèvre *et al.*, GSI Sci. Rep. 2001, GSI 2002-1, p.32.

[16] U.A. Wiedemann, U. Heinz, Phys. Rep. **319**, 145 (1999).

[17] C. Schwarz *et al.*, Nucl. Phys. A **681**, 279c (2001).

[18] M.A. Lisa *et al.*, Phys. Rev. Lett. **71**, 2863 (1993).

[19] C. Cavata *et al.*, Phys. Rev. C **42**, 1760 (1990).

[20] O. Lopez *et al.*, Phys. Lett. B **315**, 34 (1993).

[21] D. Durand *et al.*, Phys. Lett. B **345**, 397 (1995).

[22] V.K. Rodionov *et al.*, Nucl. Phys. A **700**, 457 (2000).

[23] G. Wang *et al.*, Phys. Rev. C **60**, 014603 (1999).

[24] S.E. Koonin, Phys. Lett. B **70**, 43 (1977).

[25] F. Rami *et al.*, Phys. Rev. Lett. **84**, 1120 (2000).

[26] W. Reisdorf *et al.*, GSI Sci. Rep. 2002.